Journal of Nuclear Medicine, published on September 15, 2016 as doi:10.2967/jnumed.116.180463

Enhancing expression of functional human sodium iodide symporter and somatostatin receptor in recombinant oncolytic vaccinia virus for *in vivo* imaging of tumors.

Authors: Jiahu Wang[1], Rozanne Arulanandam[1], Richard Wassenaar[2], Theresa Falls[1], Julia Petryk[2], Judith Paget[1], Kenneth Garson[1], Catia Cemeus[1], Barbara C. Vanderhyden[1,4], R. Glenn Wells[2], John C. Bell[1,3]*, Fabrice Le Boeuf[1]*#

Affiliations: [1]Centre for Innovative Cancer research; Ottawa Hospital Research Institute
Ottawa, ON, KlH 8L6; Canada

[2]Cardiac PET Research; University of Ottawa Heart Institute
Ottawa, ON K1Y 4W7; Canada

[3]Department of Biochemistry, Microbiology and Immunology; University of Ottawa
Ottawa, ON K1H 8M5; Canada

[4]Department of Cellular and Molecular Medicine; University of Ottawa
Ottawa, ON K1H 8M5; Canada

#Corresponding author: F. Le Boeuf, Ottawa Hospital Research Institute, Phone:(613)737-8899/73527, Fax:(613)247-3524. E-mail: fleboeuf@ohri.ca

*: Equal contribution.

Running title: **Vaccinia virus encoding hNIS or hSSR2**

Word Count: 5238

ABSTRACT

Purpose: Oncolytic virus (OV) therapy has emerged as a novel tool in our therapeutic arsenals for fighting cancer. As a live biological agent, oncolytic virus has the ability to target and selectively amplify at the tumor sites. We have reported that a vaccinia-based OV (Pexa-Vec) has shown good efficacy in pre-clinical models and in clinical trials. In order to give an additional tool to clinicians to allow both treatment of the tumor and improved visualization of tumor margins, we developed new viral based platforms with two specific gene reporters.

Methods: We have incorporated the human sodium iodide symporter (hNIS) and the human somatostatin receptor 2 (hSR) in the vaccinia-based OV and tested viral constructs for their abilities to track and treat tumor development in vivo.

Results: Early and high level expression of hNIS is detrimental to the recombinant virus, leading to the aggregation of hNIS protein and early cell death. Putting hNIS under a late synthetic promoter allows a higher functional expression of the protein and much stronger ^{123}I or ^{99}Tc uptake. *In vivo*, the hNIS-containing virus infects and amplifies in the tumor site, showing a better efficacy than the parental virus. The hNIS expression at the tumor site allows for the imaging of viral infection and tumor regression. Similarly, hSR-containing OV vaccinia infects and lyses cancer cells.

Conclusion: When tumor-bearing mice were given hNIS- and hSR-containing OV, radio-isotopes of ^{99}Tc and ^{111}In signals coalesce at the tumor, highlighting the power of using these viruses for tumor diagnosis and treatment.

INTRODUCTION

Diagnosing and treating cancer remain big challenges for clinicians and researchers. Early tumor diagnosis and sensitive imaging of tumor locations provides valuable insight into disease progression and may facilitate determination of the appropriate therapeutic approach to maximize treatment efficacy. Recent preclinical and clinical research has demonstrated oncolytic viral therapy as a promising alternative in fighting cancer (*1-4*). Oncolytic viruses are commonly based on engineered viruses that are attenuated, armed and/or retargeted (*4, 5*). Poxvirus, particularly vaccinia virus (VV) has been shown to be a good candidate.

The poxvirus genome can be easily genetically modified to accommodate inserts as large as 25 kb, using strategies that are dependent upon homologous recombination (*6*). Using these approaches, poxvirus family members have proven to be valuable vectors for gene therapy in a number of therapeutic applications (*7-16*), and have shown promise as novel vaccines against such diseases as acquired immunodeficiency syndrome (*18*), malaria (*19*), tuberculosis (*20*), and cancer (*7, 8, 12, 13*). Oncolytic vaccinia is known to infect a wide range of cells but only productively replicate in cancer cells with a persistent viral gene expression (*21-23*). Exploiting the vaccinia late promoter for the expression of genes of interest may provide the opportunity to maintain expression of the transgene over several days specifically in the tumor environment where viral replication is favored. Therefore, VV could be the platform of choice to express specific gene(s) that localize to and allow visualization of evolving tumors.

Two genes of potential interest for expression in the vaccinia platform were: 1) the sodium/iodide symporter (NIS) (*24*) and 2) the Somatostatin receptor type 2 (SSR2) (*25*). The use of NIS expression has been extensively used for imaging in combination with radiolabeled Technetium-99 or Iodine-131. *NIS* has been exploited therapeutically in thyroid related disease,

and ectopic expression of this gene has also been important to extend the use of radioiodine for non-thyroid tumors (*26, 27*). Notably, previous studies reported the use of measles virus as a platform expressing *NIS* and, research that has led to a current phase 1 clinical trial for ovarian cancer (*28*). SSR2 is a member of the superfamily of somatostatin receptors whose ligand is the peptide hormone somatostatin (*29*). Interestingly, somatostatin has also been shown to inhibit proliferation of many solid tumors, notably pancreatic cancer using a somatostatin analog. sandostatin or octreoide acetate has been widely used in treating carcinoid tumors (*30*).

Here we describe the construction of two new recombinant VV harboring *hNIS* or hSSR2 as *in vivo* tumor imaging candidates *and* as cancer therapeutic candidates. Our data indicate that high-level expression of hNIS and hSSR2 in recombinant VV from the early promoter leads to lower viral titers. In addition, the late promoter, although considered weaker than the early promoter, led to higher levels of hNIS expression on the membrane of the infected cells. Consequently, the uptake of iodide and technetium is also greatly improved using a late promoter in recombinant vaccinia vectors. Imaging/therapeutic virus candidates were found to preferentially replicate in various tumor sites *in vivo* and can be clearly mapped using MicroSPECT/CT without affecting normal tissues. hNIS-encoding virus has also been shown effective at killing tumor cells *in vivo*, suggesting a possible role as a therapeutic agent. Our results strongly suggest that these novel vaccinia recombinants expressing hNIS or hSRR2 may be useful to localize, visualize, follow and treat various types of tumor and warrant further investigation in a clinical setting.

MATERIALS AND METHODS

Antibodies and reagents

Primary mouse and rabbit anti-hNIS (Abcam, Canada), anti-hSSR2 (Novus Biologics, US), Ki67 (DAKO, Canada), VV Quartett (Quartett, Germany), anti-β-actin (Sigma, US). Secondary antibodies were conjugated to horseradish peroxidase (BioRad, US) or to Cy5 (Abcam, Canada) for use in immunoblotting and immunofluorescence, respectively.

Immunohistochemistry staining

Quartett IHC: Anti-vaccinia polyclonal antibody and secondary antibody kit (Vectastain, Vector Laboratories, Burlingame, CA) were used for IHC.

KI67 IHC: paraffin-embedded sections were boiled in 10mmol/l citrate buffer, pH 6. Primary anti-Ki67 antibody (1:25 dilution; DAKO) was applied overnight and detected using anti-rat antibody detection system (DAKO).

Cells

From ATCC: human osteosarcoma (U2OS), human colorectal (HT29, HCT116), human renal cell adenocarcinoma (768-O), and human breast cancer (HeLa, MCF-7). Cell lines were maintained in Dulbecco's modified Eagle's medium (Hyclone) supplemented with 10% fetal calf serum (Cansera), penicillin (100 U/ml), and streptomycin sulfate (100 μg/ml) at 37°C in 5%CO_2.

Plasmids

Plasmids pSC65-EGFP-p7.5-hNIS and -hSR, were constructed based on pSEL-eGFP (*22*) (gift from Dr. Bartlett, Pittsburgh University). Primers for late promoter sequences (Table1) were annealed and ligated to form pSC65-EGFP-p00/p04-hNIS and pSC65-EGFP-p00/p04-hSR.

Primers for late promoter construction:

P00(forward): agcttACAAAAAAAACTTCTCTAAATAGAc;

P00(reverse): tcgagTCTATTTAGAGAAGTTTTTTTTGTa;

P04(forward): agcttACAAAAAAAACTTCTCCAAATAGAc;

P04(reverse): tcgagTCTATTTGGAGAAGTTTTTTTTGTa

Recombinant viruses were constructed as previously described (*6*)

In vivo animal model

HT29 (3x10e6) tumors were established subcutaneously in 6-week-old CD1 female nude mice (*N*=5). Palpable tumors formed within 11 days after seeding. VV-eGFP or VV-hNIS were administered (1x10e7pfu/mouse). *Efficacy studies:* HT29 tumors were treated and measured every 2–4 days using an electronic caliper. Tumor volume was calculated as $(L_1)^2xL_2/2$. Ovarian cancer model, T-Antigen-positive tgMISIIR-TAg (Tg(Amhr2-SV40TAg)1Bcv) female transgenic mice (*31*) were treated with weekly i.p. injections of PBS or $1x10^8$p.f.u. control and hNIS-containing VV starting at 10 weeks of age. Mice survival times were recorded.

In vivo GFP detection

VV-infected mice were put into sleep using isoforane. The bioluminescence was detected using a 200 Series IVIS Imager (Xenogen) and Living Image® v2.5 software.

Fluorescence microscopy. To detect hNIS production from recombinant VV, U2OS cells ($2x10^5$) were seeded and infected with virus (MOI=0.01) for two days. The cells were washed (PBS) and fixed (4%paraformaldehyde) for 10min. The cells were treated for 30min with blocking buffer (0.2%Triton X-100, 5% goat serum) and incubated overnight at 4°C (1:100 anti-hNIS). The cells were washed with PBS, incubated for 30min (Cy3–conjugated goat anti-rabbit), washed (3x), mounted on a slide. DNA was stained with 1.5µg/mL 4,6-diamidino-2-

phenylindole (DAPI). Cell images were captured using a Zeiss Axioplan-2 microscope equipped with Axioview 3.1 software.

Virus DNA extraction, PCR and Sequencing

DNA was extracted from purified virus stocks by adding a lysis buffer (5mM Tris pH8.0, 2.5%Tween-20, 2.5%NP-40, 250mg/mL proteinaseK) followed by incubation at 55°C for 4hr. Samples were boiled 10min and DNA purified by phenol extraction. Regions spanning the thymidine kinase gene were amplified by PCR and sequenced to confirm the virus harboring the intended inserts.

Western blotting

Cells were infected, washed with PBS and lysed with mammalian cell lysis buffer or ProteoJET membrane protein extraction buffer (Fermentas) with protease inhibitors (Complete®, Roche) for 30min on ice. Cell lysates were sonicated for 30s, centrifuged 10,000*g* and cell pellets discarded, fractionated by electrophoresis on a Nupage 4-12% Bis-Tris gel (Invitrogen), transferred to hybond-C extra nitrocellulose membranes (Amersham), and probed with the indicated primary antibodies. Secondary antibodies conjugated to horseradish peroxidase were used to detect bound antigens.

In-vitro radioactive Isotope uptake

U2OS cells were seeded in 12-well plate at $2x10^5$ cells per well. 24hrs later, cells were infected with VV at MOI 0.1. 2 days post infection; cells were washed once with 1ml of pre-warmed (37°C) HBSS (Invitrogen). Cells were then incubated with 0.9 ml of warm HEPES (10mM) buffered HBSS and 0.1ml of ^{125}I solution (~10μCi or ~100,000cpm) for 45min at 37°C. As control, a subset of samples infected with the NIS-expressing viruses were incubated with 0.8ml of warm HEPES-HBSS, 0.1ml of 100mM potassium perchlorate ($KClO_4$) and 0.1 ml of the ^{125}I

solution. Cells were washed twice with 1ml of ice cold HEPES-HBSS before being lysed with 1ml, 1N NaOH for 15mi. ^{125}I radioactivity of the cell lysates was measured by a Gamma counter and presented in cpm per $1x10^5$ cells on average over triplicates.

Micro-SPECT imaging

Images were acquired on a 4-head small-animal SPECT/CT camera (NanoSPECT, Mediso). A 9-hole 1-mm diameter multi-pinhole collimator was attached to each head. For all studies, a spiral CT (45kVp, 500mAs/projection) was acquired to assist with localization of the radiotracer distributions. The expression of NIS was visualized through uptake of ^{99m}Tc-pertechnetate ($NaTcO_4$). Imaging was acquired with a 140+/-14keV-energy window starting 30min after a 2-2.5mCi (75-95 MBq) intra-peritoneal injection of pertechnetate. Images were acquired over 30-60 min. To image SSR2, 300mCi (11MBq) or 700mCi (26MBq) of ^{111}In-octreotide was injected intra-venously. Images were acquired for 30-60min starting 24hrs post-injection using energy windows over the two photopeaks: 173+/-17keV and 245+/-25keV. In the dual-isotope images, both ^{99m}Tc and ^{111}In images were acquired simultaneously providing exact co-registration. For the ^{131}I therapy study, 1mCi (37 MBq) of ^{131}I was injected intra-peritoneally once per week for three weeks. A pertechnetate image was obtained prior to the ^{131}I injection to evaluate the presence of NIS expression in the tumor.

Animal Care:

All animals were handled in strict accordance with good animal practice as defined by the relevant national and local animal welfare bodies, and all animal work was approved by the appropriate committee (University of Ottawa, Animal Care Committee, ME-220 protocol, Dr. John Bell).

RESULTS

Recombination of hNIS and hSSR2 with Vaccinia Wyeth strain.

Wyeth VV strain with loss of the Thymidine Kinase (TK) gene were shown to have significantly decreased pathogenicity compared to wild type virus and more specificity to tumor tissues. This vaccinia locus was chosen for insertion of the human sodium iodide symporter (hNIS) or the somatostatin receptor-2 (hSSR2). The target insertion site for hNIS and hSSR2 is shown in a schematic of the shuttle vector generated for recombination into the VV-TK locus **(Figure 1A and 2A)**. As hNIS and hSSR2 recombinant viruses are intended for imaging the productive infection at tumor sites, late expression of hNIS is more desirable for a stronger expression in the cells. Besides the early and late promoter p7.5, we have also expressed the hNIS and the hSSR2 with a synthetic late promoter p00, and p04. Selected viral plaques are depicted in *supplemental Figure 1* and show no obvious difference in term of size compared to parental virus used to make recombinants. After a GFP flow cytometer-based selection, viruses were plaque purified multiple times.

The expression of hNIS from recombinant viruses was determined in both infected cancer cells (Hela) and normal cells (GM38) **(Figure 1B-C)**. First, VV-hNIS utilizing either the p00 or p04 late promoters shows strong tropism for tumor cells based on the enhanced expression of GFP **(Figure 1B)**, the higher virus titers **(Figure 1C)** and the enhanced expression of hNIS **(Figure 1D)** in the tumor cell line when compared to normal cells. While specific hNIS expression was confirmed and as expected accordingly to the literature by western blot **(Figure 1D)** (*32*) (*33*) (*34*), the functionality of the symporter was validated by measuring the accumulation of iodine-131 or Technetium-99 radioisotopes into the cells **(Figure 1E-F)**. This accumulation is NIS specific as $KClO_4$ can block the uptake. hNIS driven by late promoters again are found to be

more active than expression from the early late p7.5 promoter when cells were infected with the same MOI **(Figure 1E)**.

In parallel, expression of hSSR2 from recombinant VV-hSSR2 viral constructs was validated by immunofluorescence **(Figure 2B-C)**. Specific staining for SSR2 in infected cells (GFP expressing) confirmed both expression and localization of SSR2 **(Figure 2B-C)**. Interestingly, using an early/late promoter (p7.5) or a late promoter (p04) changed the localization of SRR2. In fact, aggregation was observed with the early/late promoter and, a more homogenous distribution suggesting a better functionality was observed using a late vaccinia promoter **(Figure 2C)**.

Late promoter hNIS encoding virus can infect and lyse cancer cells

hNIS oncolytic virus candidates were tested in vitro and vivo for their ability to spread in tumor cells and their therapeutic potential. First, we observed that hNIS virus can infect and replicate in various type of human tumor cells: colon carcinoma HT29 and HCT116, renal carcinoma 786-O, osteosarcoma U2OS or breast tumor cells **(Figure 3A and C)** leading to high ectopic expression of hNIS **(Figure 1B)**. As expected, VV-hNIS platforms incorporating the late promoters p00 or p04, replicate in the subcutaneous human HT-29 immuno compromised mouse tumor model as demonstrated by viral eGFP expression assessed by in-vivo imaging system (IVIS) **(Figure 3D)**. Vaccinia virus expression in tumors was confirmed after the sacrifice of animals by 1) assessing the viral expression of eGFP directly by microscopy and 2) by immunohistochemistry staining for vaccinia antigens **(Figure 3E)**. Interestingly, we also performed an immunohistochemistry staining to assess proliferating cells **(Figure 3E)**. We observed that regions showing vaccinia-infected cells resulted in dead tissue without any evidence of proliferating tumor cells. Confirming that these viruses may be controlling tumor

growth, the parental vaccinia virus and the hNIS expressing derivatives were all able to significantly control the growth of the tumor and to increase the overall survival of the treated mice compared to the PBS control group **(Figure 3F-G)**.

hNIS encoding virus can be imaged using SPECT/CT.

In order to validate in vivo imaging using ^{99}Technetium (^{99}Tc), ^{99}Tc tracer was injected four days after the intratumoral treatment of human HT29 xenografted tumors either PBS control, parental vaccinia virus or hNIS-recombinant virus. After one hour to allow the tracer to reach all organs, mice were imaged using microSPECT/CT **(Figure 4A-C)**. Consistent with an earlier reports, the thyroid, salivary gland, stomach, bladder and occasionally bowel were positive for ^{99}Tc signal **(Figure 4A)** (*35*) (*36*). However, there were no radioactive signals for tumors treated with either PBS or non-expressing hNIS virus (**Figure 4A)**. In contrast, mice treated with the hNIS-encoding oncolytic candidates showed strong positive ring shaped signals in the tumor. Interestingly, we have noted that the signal persisted for at least to 11 days after the initial viral injection (Data not shown). While these studies were initially performed with intratumor delivery of virus, intravenous delivery of virus was also found to be sufficient for in vivo imaging of tumor using microSPECT/CT (**Figure 4B**), opening the possibility of using systemic virus delivery to image tumors at remote sites. With the aim to assess the safety profile of using a viral platform expressing NIS receptor, we determined the level of virus replication, human NIS expression and radioactive tracer accumulation in various tissues from tumor-bearing and tumor-free mice (Supplemental Figure 1). At 24 hrs, 48 hrs, and 72 hrs post virus injection, ^{99m}Tc-pertechnetate was injected and normal tissues (including blood, brain, bone, muscle, stomach, bladder, thyroid, ovaries) were harvested from both tumor-free and tumor-bearing mice with the

additional tumor tissue harvested from the latter group of mice. A Gamma counter was then used to measure the radiation in each tissue (Supplemental Figure 1A). Subsequently, portions of all tissues were homogenized and membrane proteins extracted for Western blotting to assay expression of the human NIS protein (Supplemental Figure 1B). Finally, the remaining portions of the tissues were titered for Vaccinia virus (Supplemental Figure 1C). As expected, we observed a strong radiation signal in tumor in addition to a strong signal in the few normal tissues in both tumor-free or tumor-bearing mice that are known to express endogenous murine NIS (thyroid, bladder and stomach). Consistent with these finding, the virus was only detected in high amounts in tumor tissues (Supplemental Figure 1C). This observation matched perfectly with the western blotting, where expression of human NIS was only seen in the tumor tissue. In conclusion, based on tissue viral titres, significant amounts of virus replication occurs primarily in the tumor tissue. This correlates well with our ability to detect the virus encoded human NIS protein only in tumor tissue and with the observation that the only tissues that accumulated the pertechnetate radiotracer, other than tissues known to express endogenous murine NIS, were the tumor tissues.

In parallel, the octreotide radiolabeled with ^{111}Indium, a drug already in clinic use, was similarly effective for imaging tumor infected with virus candidates expressing hSSR2 **(Figure 4C)**. As expected, results mirrored those obtained with hNIS expressing vaccinia and tumor labeling with ^{99}Tc was observed confirming the potential of this viral technology to be used for both imaging as well as anti-tumor therapeutic.

hNIS encoding virus is able to infect and localize multiple tumors by imaging.

The murine tgMISIIR-Tag, a T-antigen driven ovarian cancer model, makes several foci of tumor development in the ovaries and is an extremely difficult model to cure. We tested vaccinia hNIS viral platform for imaging tumors in this model to assess the potential of this new therapeutic candidate (Figure 5A). Interestingly, the systemic injection of the VV-hNIs virus revealed clear imaging of multiple tumor nodules in the tumor bearing mice in vivo, using ^{99}Tc. Replication of vaccinia in this model was evident by imaging of GFP expression in excised ovarian tumors (Figure 5C). A survival study using the same ovarian tumor model (Figure 5B) showed enhanced survival of mice that received the hNIS virus with I131 when compared to I131 treatment alone. Together, these data strongly suggest 1) the potential clinical use of viruses expressing symporter in combination with radioisotopes to localize and visualize tumor growth and, 2) the direct therapeutic potential of using viral platforms expressing symporter for treating various types of cancers.

Finally, using HT29 tumor, we examined the ability of VV-hNIS and VV-hSRR2 to replicate and also to accumulate injected radioisotopes in the tumor of a single animal (Figure 6). Four days after injections of viruses, technetium and iodide radioisotope were co-injected intra-peritoneal (^{111}In) or intra-venous (^{99}Tc) and tracer were followed by microSPECT/CT. Result shows both radioisotopes accumulation in the tumor implantation suggesting that hNIS and hSRR2 encoding viruses can both be used simultaneously for imaging.

DISCUSSION

In this study, we show the potential use of VV expressing two different genes, NIS symporter and the SSR2 receptor in the aim of visualizing and treating tumor. Using microSPECT/CT imaging system we were able to clearly visualize and localize tumor in various mouse models. Using this recombinant vaccinia expression platform, systemic administration of virus and subsequently radioisotopes led to accumulation of isotope in the tumor bed and improved survival in an ovarian cancer model.

Poxviruses continue to be important therapeutics for the prevention and treatment of human diseases. Vaccinia application for the eradication of smallpox has been one of the most important medical advances in human history providing to the scientific and medical community strong data on the safety profile of the virus. A variety of poxvirus based vaccine vectors have been developed for human infectious diseases and as agents for the treatment of cancer. This characteristic gives us the opportunity to combine two desirable effects: a cancer therapeutic and a cancer tool for tumor localization. The lytic ability of the platform has been described several times in various pre-clinical models but also in clinical trials. An important feature of this specific vaccinia viral platform is its strong ability to image the tumor after systemic injections, making this platform a very attractive prospect for mapping and imaging tumor in patients with metastatic disease. Also, due to its large genome and to its slow replication, as a viral platform, vaccinia can uniquely replicate in the tumor over the course of several days after systemic injection, giving the opportunity for recombinant gene to be expressed during a long period of time. We also show that the choice of vaccinia promoters regulating the expression of the transgenes is crucial. In fact, a late promoter, in both platforms expressing hNIS or hSSR2, is clearly more advantageous for maintained strong expression in tumor cells when compared to an

early/late promoter. Moreover, we also observe that the SSR2 localization is optimal using late promoter. The radiotracer concentration taken up in tumor nodules is critical for capturing a strong enough signal for imaging using the microSPECT/CT and is obviously extremely dependent on the level of expression of the symporter/receptor. Strongest and most functional expression of the symporter and receptor in vivo was observed when we use late vaccinia promotor p00 or p04.

Importantly, we also conducted experiments to make a strong correlation between the tracer signal, human NIS symporter membrane expression as well as viral replication. Vaccinia TK knockout virus exhibited a strong safety profile based on its persistent only in tumor. Human NIS protein expression was only detected in tumor as well and accumulation of tracer correlated with NIS-positive tumor in addition to a few normal tissues known to express endogenous murine NIS (stomach, bladder and thyroid notably). This viral dynamic suggests that vaccinia virus has strong advantages in its use to carry and selectively express membrane proteins such as NIS. Furthermore, with virus titers in normal tissues that are more than 4 orders of magnitude lower than that found in tumors, we do not expect the virus to drive sufficient amounts of NIS protein expression to make a difference in the accumulation of the tracer.

We have chosen two different VV expression platforms to allow the imaging of tumor sites in vivo: one using hNIS and the second one SSR2 transgene. These two genes operate differently and can offer complementary results when combined together. hNIS has been shown to work well in the measles virus platform and is now in clinical evaluation. Using viruses as a gene therapy platform to target cancer cells and express NIS, clearly shows promise in the treatment and visualization of tumor. Interestingly, accumulation of ^{111}In radioistopes will be only in live cells expressing NIS pump. Somatostatin receptor type 2 is surface cell receptor that

can be used as a target for specific targeted drugs. Notably, SSR2 is overexpressed in certain type of cancer. Using the ^{111}In-Octreotide, a Food and Drug Approved drug, in patients with neuroendocrine tumor, provides high-resolution images available to clinicians helping for diagnosis. Advantage of using this receptor is notably that SSR2 can be expressed on live and dead tumor cells providing a different picture area of the tumor compared of using the hNIS genes viral platform.

Route of injection of therapeutic agent can be a source of great debate; vaccinia virus expressing specific reporter genes can help in the decision and contribute to a better success in the following clinical trials when used as stand-alone or in combination with specific anticancer treatment such as checkpoint inhibitors.

CONCLUSION

Here we report the use of two new vaccinia-based viruses expressing two different imaging genes for tumor visualization and treatment. Both platforms, with their respective radiolabelled counterparts, can be used independently or together offering unique opportunities to diagnose suspected cancer, visualize multiple metastasis with high quality microSPECT/CT imaging and, to provide a treatment through the use of the oncolytic viral platform activating multiple mechanism of action against tumor.

Authors' Contributions:

Conception and design: JW,RGW,JB,FLB; Development of methodology: JW,RA,JP,CC; Imaging: RW,JP,RGW. Animal work: TF, FLB, KG. Analysis/data interpretation: JW, RA, KG, FLB. Writing, review: JW,KG,BV,JB,FLB,RGW. Supervision: RGW,JB; FLB

Grant Support

This work was supported by grants from the National Cancer Institute of Canada, Terry Fox Foundation, Natural Sciences and Engineering Research Council of Canada, and the Canadian Institutes of Health Research to JB and RGW.

REFERENCES

1. Bell JC. Interfering with tumor pathways that augment viral oncolysis. *Mol Ther.* 2011;19:2108-2109.

2. Bell JC, McFadden G. Editorial overview: Oncolytic viruses--replicating virus therapeutics for the treatment of cancer. *Curr Opin Virol.* 2015;13:viii-ix.

3. Auer R, Bell JC. Oncolytic viruses: smart therapeutics for smart cancers. *Future Oncol.* 2012;8:1-4.

4. Russell SJ, Peng KW, Bell JC. Oncolytic virotherapy. *Nat Biotechnol.* 2012;30:658-670.

5. Stojdl DF, Lichty BD, tenOever BR, et al. VSV strains with defects in their ability to shutdown innate immunity are potent systemic anti-cancer agents. *Cancer Cell.* 2003;4:263-275.

6. Rintoul JL, Wang J, Gammon DB, et al. A selectable and excisable marker system for the rapid creation of recombinant poxviruses. *PLoS One.* 2011;6:e24643.

7. Mastrangelo MJ, Maguire HC, Jr., Eisenlohr LC, et al. Intratumoral recombinant GM-CSF-encoding virus as gene therapy in patients with cutaneous melanoma. *Cancer Gene Ther.* 1999;6:409-422.

8. Erbs P, Findeli A, Kintz J, et al. Modified vaccinia virus Ankara as a vector for suicide gene therapy. *Cancer Gene Ther.* 2008;15:18-28.

9. Smith GL, Mackett M, Moss B. Infectious vaccinia virus recombinants that express hepatitis B virus surface antigen. *Nature.* 1983;302:490-495.

10. Smith GL, Murphy BR, Moss B. Construction and characterization of an infectious vaccinia virus recombinant that expresses the influenza hemagglutinin gene and induces resistance to influenza virus infection in hamsters. *Proc Natl Acad Sci U S A.* 1983;80:7155-7159.

11. Cadoz M, Strady A, Meignier B, et al. Immunisation with canarypox virus expressing rabies glycoprotein. *Lancet.* 1992;339:1429-1432.

12. Kantoff PW, Schuetz TJ, Blumenstein BA, et al. Overall survival analysis of a phase II randomized controlled trial of a Poxviral-based PSA-targeted immunotherapy in metastatic castration-resistant prostate cancer. *J Clin Oncol.* 2010;28:1099-1105.

13. Harrop R, Drury N, Shingler W, et al. Vaccination of colorectal cancer patients with modified vaccinia ankara encoding the tumor antigen 5T4 (TroVax) given alongside chemotherapy induces potent immune responses. *Clin Cancer Res.* 2007;13:4487-4494.

14. Dasgupta S, Bhattacharya-Chatterjee M, O'Malley BW, Jr., Chatterjee SK. Recombinant vaccinia virus expressing interleukin-2 invokes anti-tumor cellular immunity in an orthotopic murine model of head and neck squamous cell carcinoma. *Mol Ther.* 2006;13:183-193.

15. Lorenz MG, Kantor JA, Schlom J, Hodge JW. Anti-tumor immunity elicited by a recombinant vaccinia virus expressing CD70 (CD27L). *Hum Gene Ther.* 1999;10:1095-1103.

16. Lorenz MG, Kantor JA, Schlom J, Hodge JW. Induction of anti-tumor immunity elicited by tumor cells expressing a murine LFA-3 analog via a recombinant vaccinia virus. *Hum Gene Ther.* 1999;10:623-631.

17. Evgin L, Vaha-Koskela M, Rintoul J, et al. Potent oncolytic activity of raccoonpox virus in the absence of natural pathogenicity. *Mol Ther.* 2010;18:896-902.

18. Kanesa-thasan N, Smucny JJ, Hoke CH, et al. Safety and immunogenicity of NYVAC-JEV and ALVAC-JEV attenuated recombinant Japanese encephalitis virus--poxvirus vaccines in vaccinia-nonimmune and vaccinia-immune humans. *Vaccine.* 2000;19:483-491.

19. Bejon P, Ogada E, Mwangi T, et al. Extended follow-up following a phase 2b randomized trial of the candidate malaria vaccines FP9 ME-TRAP and MVA ME-TRAP among children in Kenya. *PLoS One.* 2007;2:e707.

20. Huygen K, Content J, Denis O, et al. Immunogenicity and protective efficacy of a tuberculosis DNA vaccine. *Nat Med.* 1996;2:893-898.

21. Parato KA, Breitbach CJ, Le Boeuf F, et al. The oncolytic poxvirus JX-594 selectively replicates in and destroys cancer cells driven by genetic pathways commonly activated in cancers. *Mol Ther.* 2012;20:749-758.

22. McCart JA, Ward JM, Lee J, et al. Systemic cancer therapy with a tumor-selective vaccinia virus mutant lacking thymidine kinase and vaccinia growth factor genes. *Cancer Res.* 2001;61:8751-8757.

23. Le Boeuf F, Diallo JS, McCart JA, et al. Synergistic interaction between oncolytic viruses augments tumor killing. *Mol Ther.* 2010;18:888-895.

24. Micali S, Bulotta S, Puppin C, et al. Sodium iodide symporter (NIS) in extrathyroidal malignancies: focus on breast and urological cancer. *BMC Cancer.* 2014;14:303.

25. Appetecchia M, Baldelli R. Somatostatin analogues in the treatment of gastroenteropancreatic neuroendocrine tumours, current aspects and new perspectives. *J Exp Clin Cancer Res.* 2010;29:19.

26. De La Vieja A, Dohan O, Levy O, Carrasco N. Molecular analysis of the sodium/iodide symporter: impact on thyroid and extrathyroid pathophysiology. *Physiol Rev.* 2000;80:1083-1105.

27. Riesco-Eizaguirre G, Santisteban P. A perspective view of sodium iodide symporter research and its clinical implications. *Eur J Endocrinol.* 2006;155:495-512.

28. Galanis E, Atherton PJ, Maurer MJ, et al. Oncolytic measles virus expressing the sodium iodide symporter to treat drug-resistant ovarian cancer. *Cancer Res.* 2015;75:22-30.

29. Liu Y, Lu D, Zhang Y, Li S, Liu X, Lin H. The evolution of somatostatin in vertebrates. *Gene.* 2010;463:21-28.

30. Grimberg A. Somatostatin and cancer: applying endocrinology to oncology. *Cancer Biol Ther.* 2004;3:731-733.

31. Garson K, Gamwell LF, Pitre EM, Vanderhyden BC. Technical challenges and limitations of current mouse models of ovarian cancer. *J Ovarian Res.* 2012;5:39.

32. Peyrottes I, Navarro V, Ondo-Mendez A, et al. Immunoanalysis indicates that the sodium iodide symporter is not overexpressed in intracellular compartments in thyroid and breast cancers. *Eur J Endocrinol.* 2009;160:215-225.

33. Huc-Brandt S, Marcellin D, Graslin F, et al. Characterisation of the purified human sodium/iodide symporter reveals that the protein is mainly present in a dimeric form and permits the detailed study of a native C-terminal fragment. *Biochim Biophys Acta.* 2011;1808:65-77.

34. Castro MR, Bergert ER, Beito TG, McIver B, Goellner JR, Morris JC. Development of monoclonal antibodies against the human sodium iodide symporter: immunohistochemical characterization of this protein in thyroid cells. *J Clin Endocrinol Metab.* 1999;84:2957-2962.

35. Wapnir IL, Goris M, Yudd A, et al. The Na+/I- symporter mediates iodide uptake in breast cancer metastases and can be selectively down-regulated in the thyroid. *Clin Cancer Res.* 2004;10:4294-4302.

36. Harun-Or-Rashid M, Asai M, Sun XY, Hayashi Y, Sakamoto J, Murata Y. Effect of thyroid statuses on sodium/iodide symporter (NIS) gene expression in the extrathyroidal tissues in mice. *Thyroid Res.* 2010;3:3.

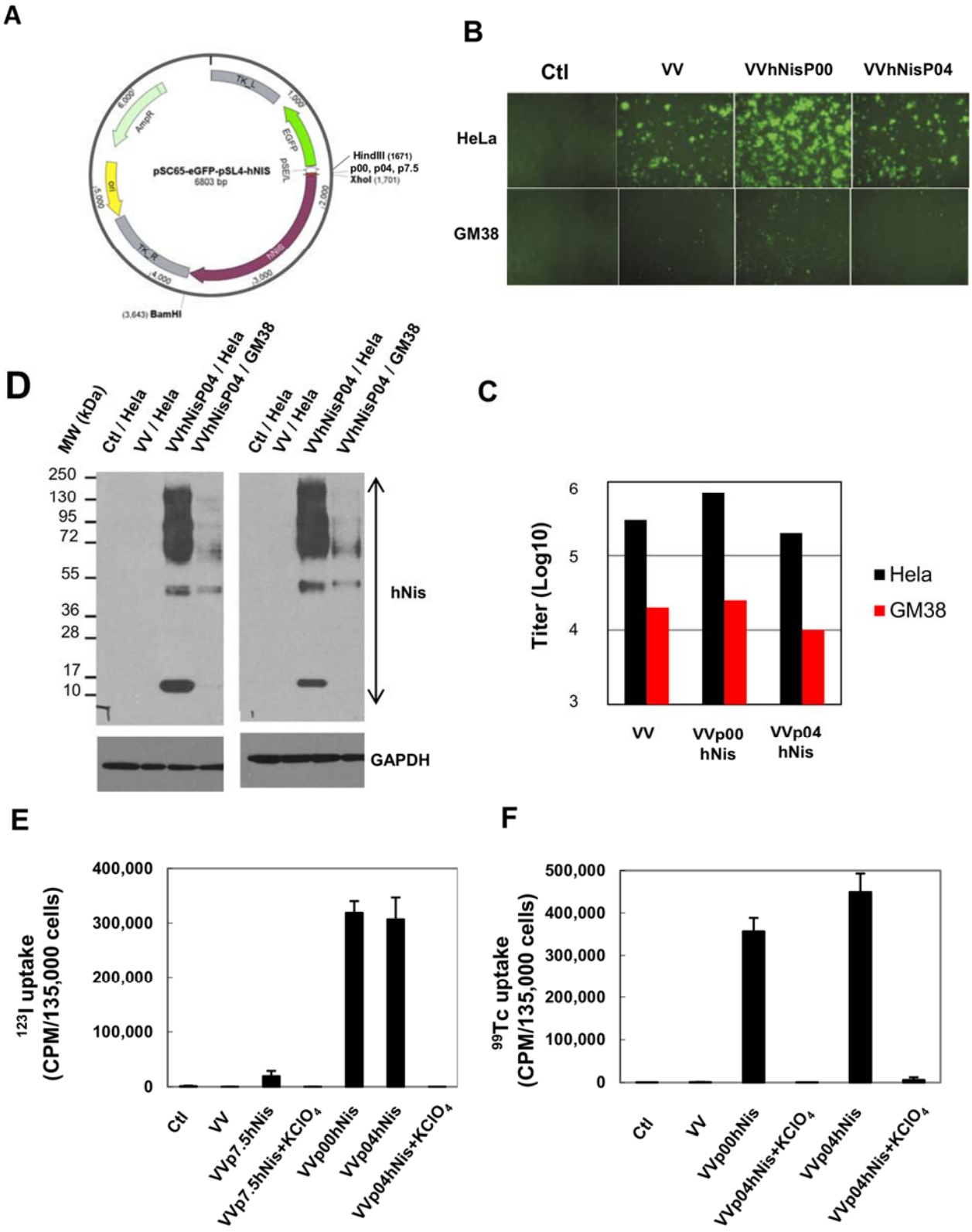

Figure 1: Late promoter allows high-level expression of functional hNIS using vaccinia-based platform, **A**. Diagram of the shuttle vector used to generate the recombinant hNIS

vaccinia virus (VV). **B**. GFP images 48hrs post-infection of Hela and GM38 uninfected (Ctl) or infected with VV, VV-NIS p00 or p04. **C**. VV titers, 48hrs after infection of HeLa, MRC5 and GM38. **D.** Western blot for NIS expression. HeLa cells were uninfected (Ctl) or infected with VV or VV-NIS p00 or p04. Sample lysate collections were done 48hrs post-infection and screened by Western blot. **E.** ^{131}I uptake of U2OS cells, uninfected (Ctl) or infected with VV, or VV-hNIS expressing recombinants. Inhibition of the hNIS symporter was achieved by treatment with $KCLO_4$. **F**. ^{99}Tc uptake of U2OS cells, uninfected (Ctl) or infected with VV, or VV-hNIS expressing recombinants. Inhibition of the hNIS symporter using $KCLO_4$.

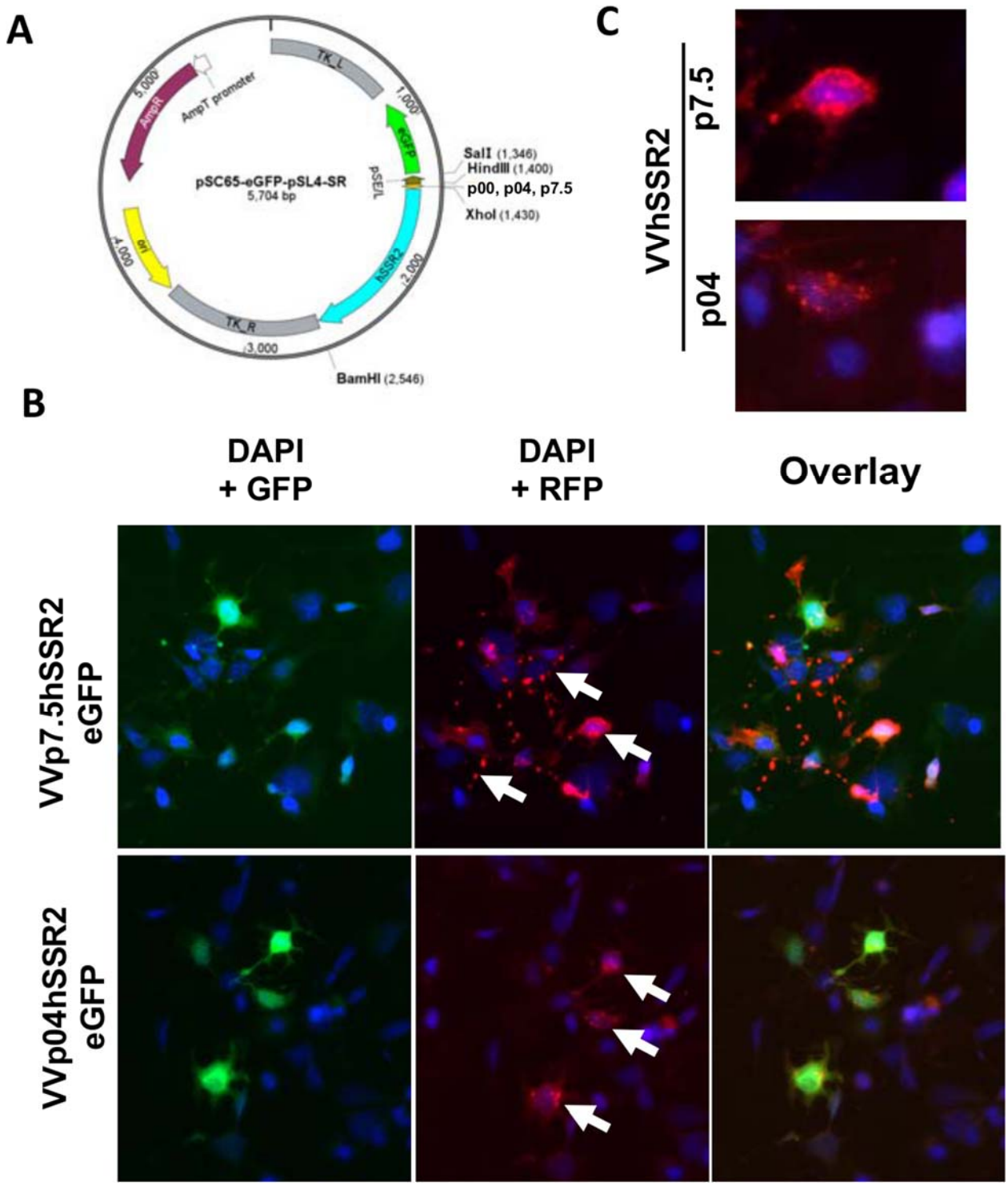

Figure 2: Late promoter for hSSR2 vaccinia-based platform expression, **A** Diagram of the vector used to generate the recombinant VV-hSSR2. **B.** Immunofluorescence of U2OS cells infected by early/late p7.5 VV-hSRR2 and late p04. Arrows point out localization of hSSR2:

more cytoplasmic homogenously distributed hSSR2 when using late promotor vs compacted expression when hSSR2 is under early/late promoter. Pink: hSSR2, Green: GFP from viral gene expression, blue: DAPI, **C.** Magnified view of specific cells with immunofluorescence staining.

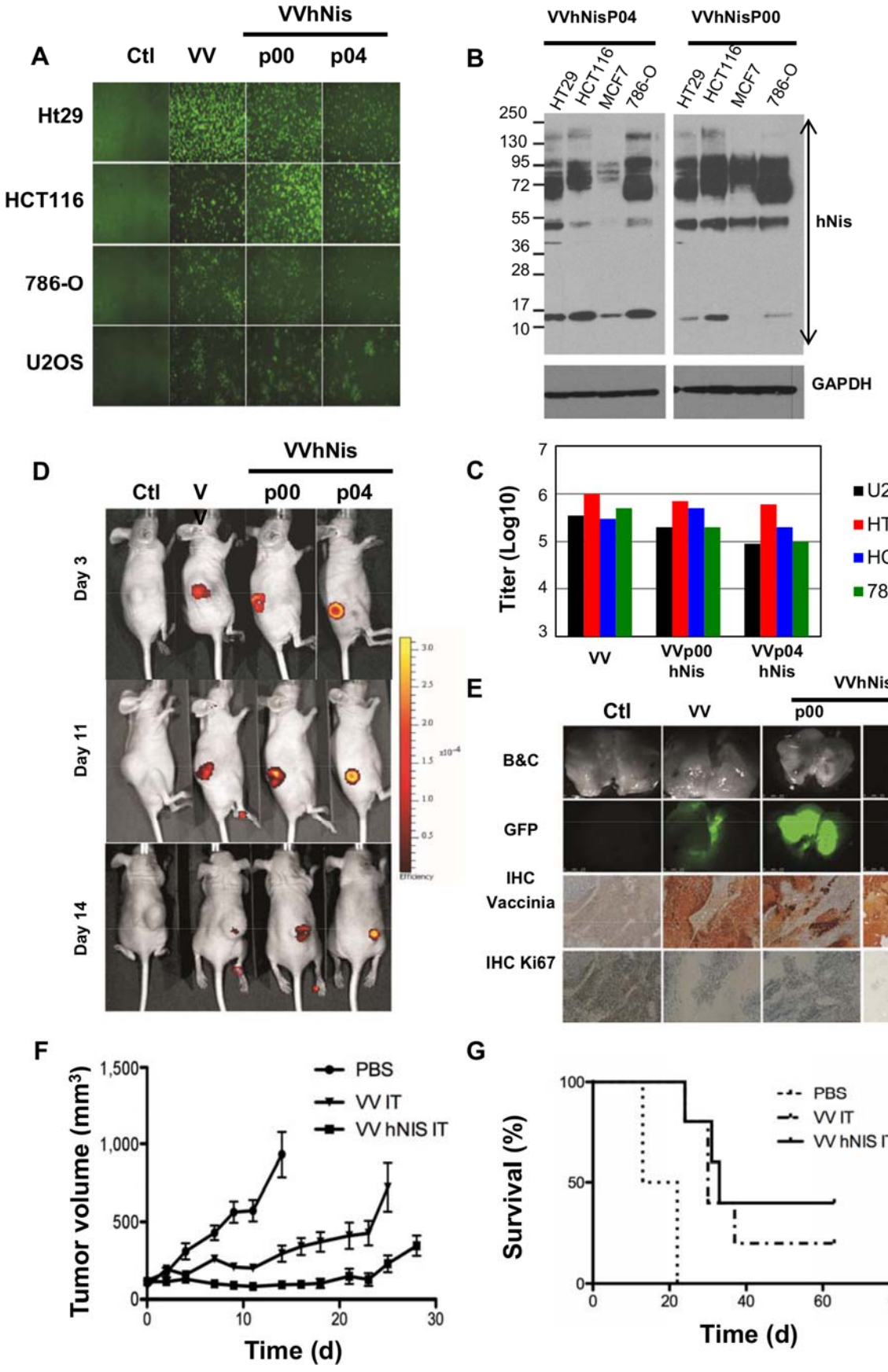
A
Ctl
VV
VVhNis
p00
p04
Ht29
HCT116
786-O
U2OS
B
VVhNisP04
VVhNisP00
HT29
HCT116
MCF7
786-O
250
130
95
72
55
36
28
17
10
hNis
GAPDH
C
Titer (Log10)
7
6
5
4
3
U2OS
HT29
HCT116
786-O
VV
VVp00 hNis
VVp04 hNis
D
Ctl
V
VVhNis
p00
p04
Day 3
Day 11
Day 14
E
Ctl
VV
VVhNis
p00
p04
B&C
GFP
IHC Vaccinia
IHC Ki67
F
Tumor volume (mm³)
1,500
1,000
500
0
PBS
VV IT
VV hNIS IT
0
10
20
30
Time (d)
G
Survival (%)
100
50
0
PBS
VV IT
VV hNIS IT
0
20
40
60
80
Time (d)

Figure 3: In vitro and in vivo infection of tumor cell with hNIS-encoding viruses, A. GFP-images (48h post-infection) of HT29, HCT116, 786-O, U2OS either uninfected (Ctl) or infected with VV, VV-hNIS p00 or p04 (MOI:0.01). **B**. Western blot for NIS expression in tumors cells was perform as described earlier. **C.** Viral titers (48h post-infection), **D**. HT29 tumor were established in nude mice. Ten days later, mice were treated (intra-tumor) with PBS (Ctl), VV, or VV-hNIS p00 or p04. GFP associated virus expression was monitored using IVIS, 3, 11 and 14 days after virus administration, **E**. Mice were sacrificed (day 14) and tumor harvested. Excised tumors were imaged for viral GFP expression and paraffin embedded blocks prepared from the tumors were screened by IHC for Vaccinia antigens, and Ki67. **F.** HT29 tumor volume was monitored for each group and average tumor volumes are shown (N=5). Treated groups vs PBS are significantly different ($P<0.001$). Error bars are standard error. **G.** HT29 bearing tumor mice survival was monitored over time. Log-rank test indicates that treatment with VV with or not hNIS expression significantly extended survival compared to PBS ($P<0.01$).

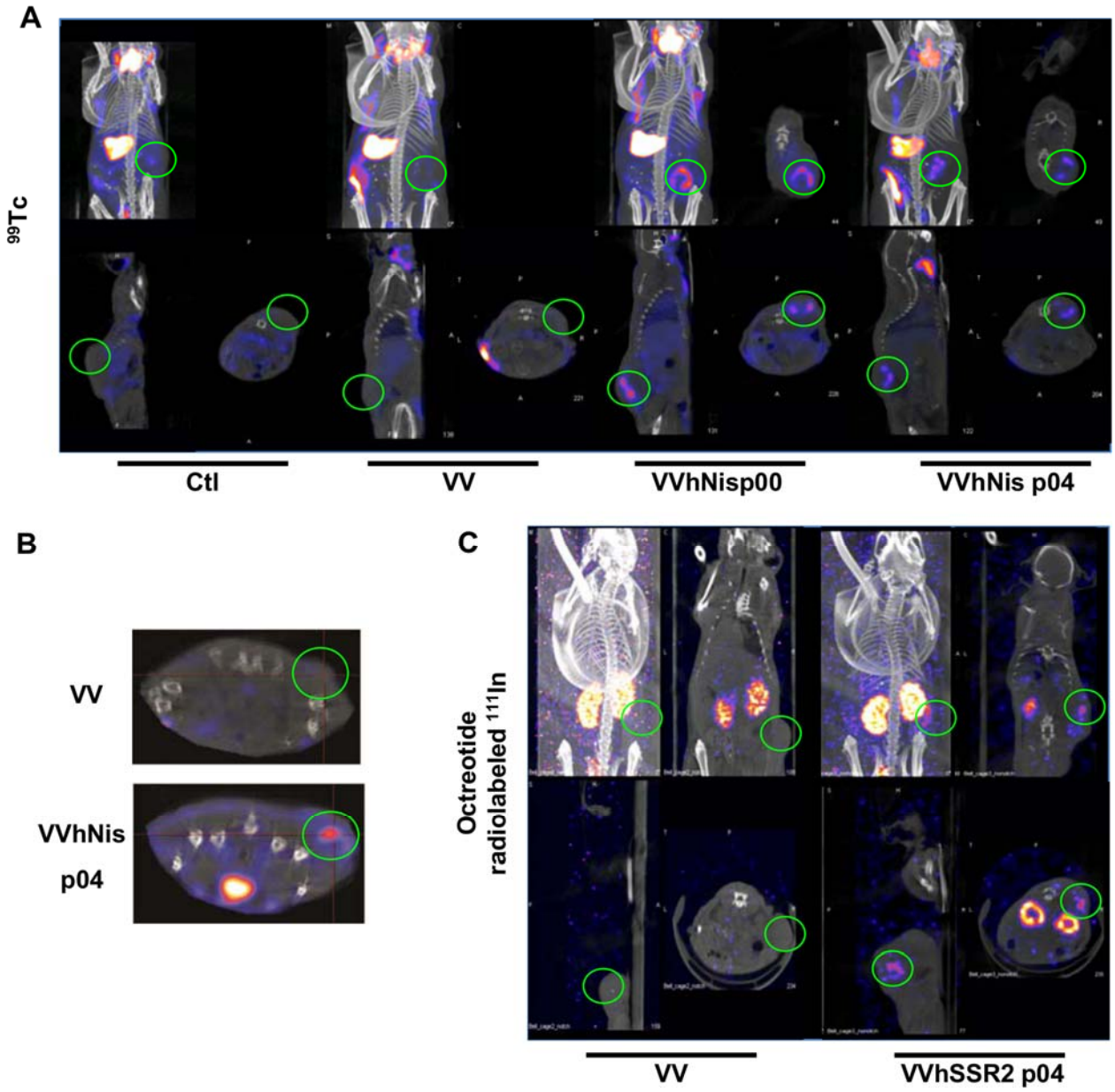

Figure 4: Radioisotope uptake for Nude mice bearing HT29 tumor treated with control, hNIS or hSSR2-encoding viruses, A. HT29 were established in sub-cutaneous in mice before intra-tumor injection with PBS (Ctl) or the indicated VV. 4 days after virus treatment, mice were injected with ^{99}Tc radioisotope for microSPECT/CT imaging, **B**. microSPECT/CT images of HT29 tumor bearing mice at day 4 post intra-venous virus delivery, **C**. HT29 tumor were

injected intra-tumor with VV or VV-hSSR2 4 days after virus treatment, mice were injected with Octreotide-^{111}In for microSPECT/CT.

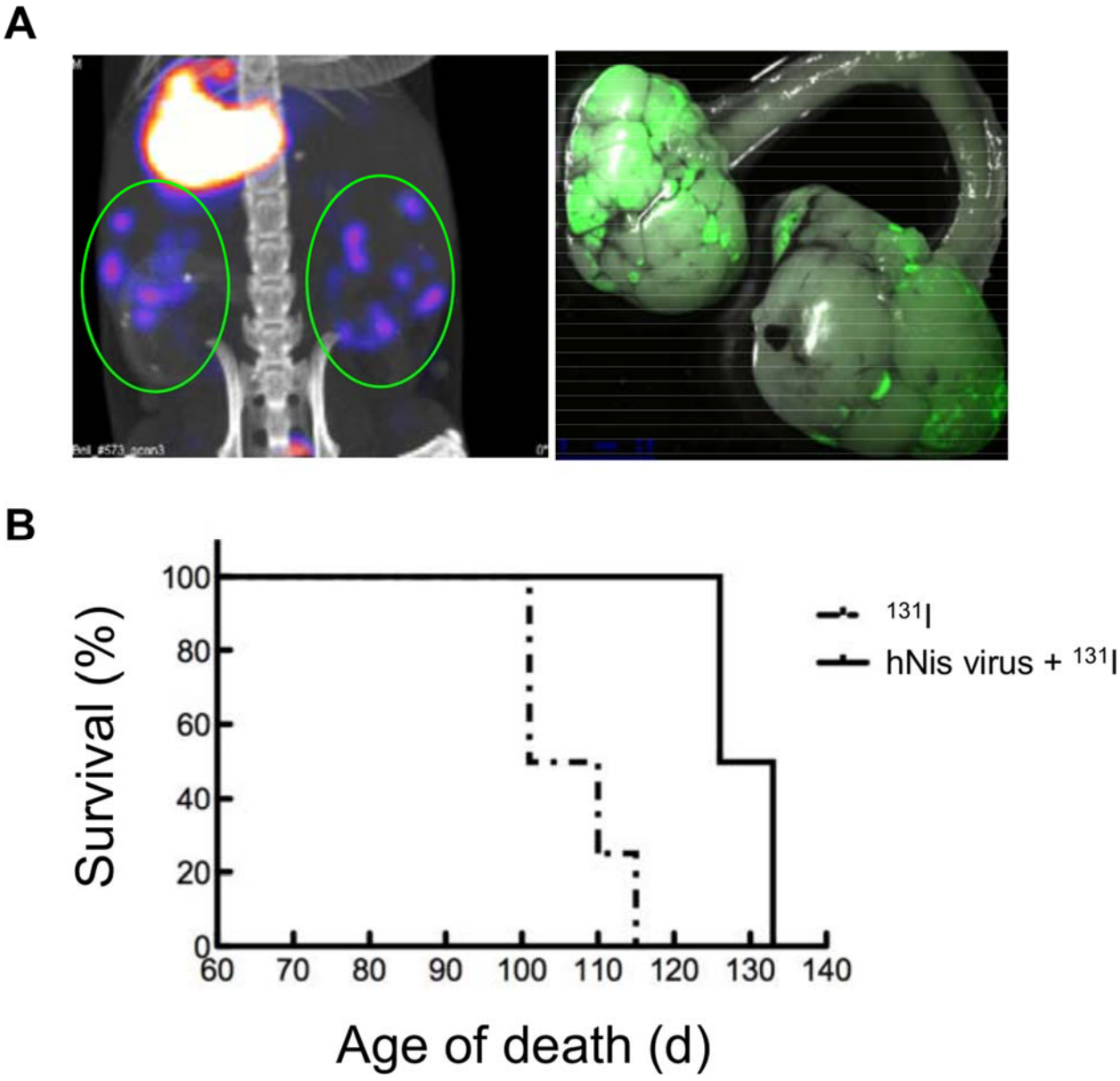

Figure 5: VV-hNIS is able to reveal and treat a transgenic ovarian tumor mouse model, A. tgMISSIIR-TAg transgenic mice were treated with VVp04-hNIS. TgMISIIR-TAg mice, 90 days of age, were injected intra-venous with VV-hNIS and 4 days later, a microSPECT/CT image was done. **B.** Survival of TgMISSIIR-Tag transgenic mice was monitored over time after treatment with VVp04-hNIS with ^{131}I (N=5).

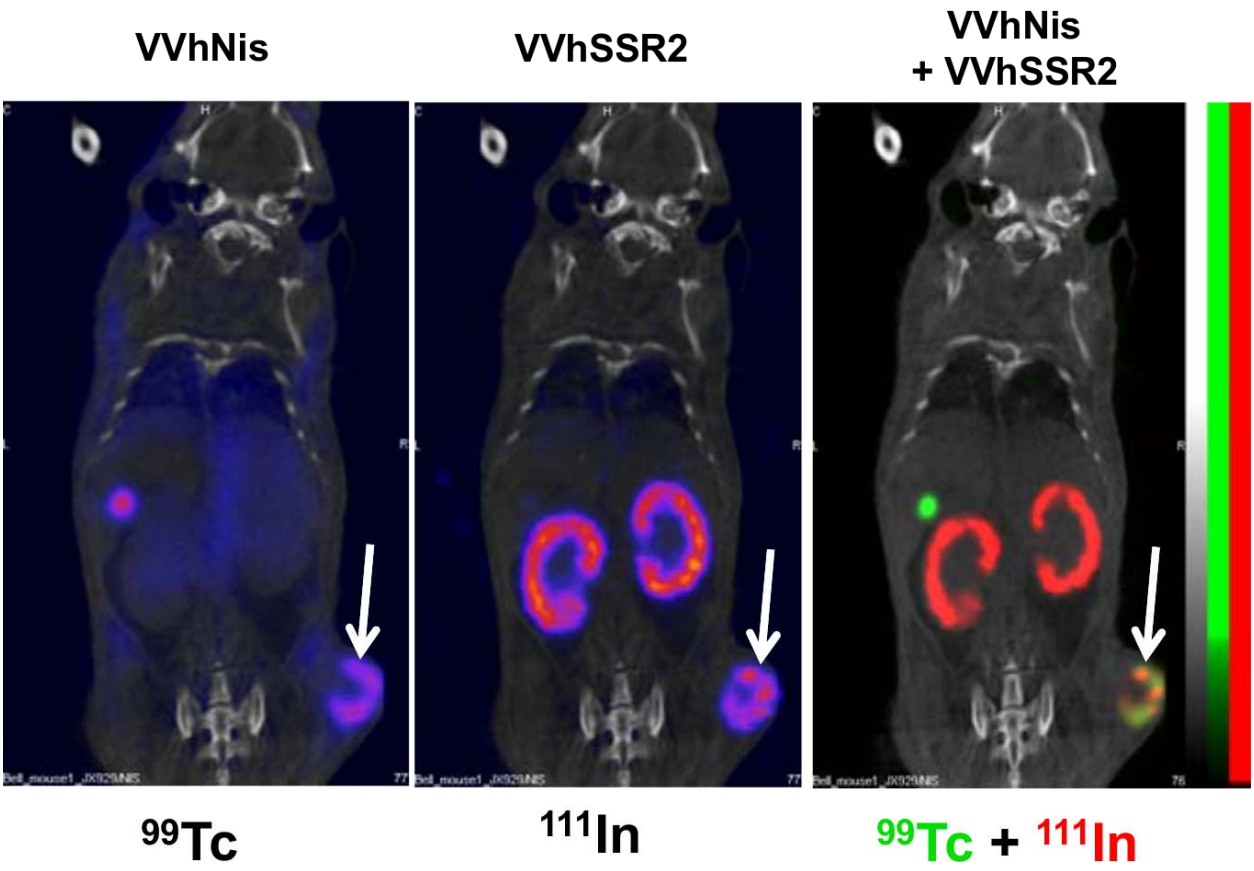

Figure 6: Dual VV-hNIS and VV-hSSR2 use to visualize and treat tumor, HT29 tumor were injected with VV-hNIS and VV-hSSR2 intra-tumor. 4 days after virus treatment, mice were injected with ^{99}Tc and ^{111}In radioisotope for microSPECT/CT imaging.